A Finite Element for Vibration Analysis of Twisted Blades Based on Beam Theory

F. Sisto* and A. T. Chang†
Stevens Institute of Technology, Hoboken, New Jersey

A finite element method of discretizing beam segments of pretwisted rotating blades is presented. Employing the matrix displacement method, stiffness and mass properties are developed from basic mechanics of a pretwisted beam theory. By introducing the proper displacement functions, the structural stiffness matrix and the effect of rotor blade rotational motion on the stiffness matrix are obtained systematically from the potential and kinetic energy functions. Comparing with other beam elements, the derivation of this element is more fundamental. This would allow one to apply the same approach to more complicated problems such as blade motions in a gyroscopic rotational field. Illustrative examples are given comparing numerical results with available data and other numerical solutions from rotating and nonrotating force fields. These examples show that accurate prediction of vibration frequencies for pretwisted blades can be obtained by employing a quite modest number of degrees of freedom.

Nomenclature

a	= arbitrary axial strain
$c_1, c_2, \ldots, c_{12}$	= polynomial constants
d	= distance of an arbitrary point from shear center
e_x, e_y	= positions of neutral axis from shear center
E	= modulus of elasticity
i, j, k	= element fixed coordinate system
ℓ_H	= length of a helical fiber under pretwist
N_i	= shape functions
s	= element coordinate
T	= kinetic energy
$\bar{u}, \bar{v}$	= bending deformations in element midplane principal directions
$u_1, v_1, w_1, \phi_1, u_2, v_2, w_2 \phi_2$	= nodal variables
u, v	= element bending deformations
U	= potential energy
w	= element axial deformation
α	= angle of pretwist per length
γ	= spiral angle of a helical fiber
$\{\epsilon\}$	= deformation strain
ξ^*, η^*	= defined in Eq. (7)
ξ_i, η_i	= nodal points defined in Eq. (16)
ξ, η, ζ	= position in element fixed coordinate system
$\{\sigma\}$	= stress
ϕ	= element torsional deformation
$\bar{\phi}$	= angle of twist per length
ω	= angular velocity of rotor

Introduction

DYNAMIC motion of rotating pretwisted blades has been studied extensively because accurate knowledge of the motion is essential in aeroelastic studies, dynamic analysis, and the design of turbomachinery, windmill, and helicopter rotors. It is beyond the scope of this paper to discuss all of the methods available in the literature. With recent advances in the finite element technique, this method is perhaps the most convenient way to analyze rotating blades. It has been shown that the behavior of a pretwisted blade can be modeled accurately by either plate or shell finite elements. Dynamics of rotating blades can even be studied by general-purpose finite element programs such as NASTRAN. However, for certain types of blade dynamic problems, such as the shrouded bladed disk and blades with complicated rotational motion, the finite element model of two-dimensional elements is either not suitable or too difficult to apply because it requires too many degrees of freedom. In these cases, the beam model is more appropriate and flexible. In particular, if the dynamic problem involves only thin, high aspect ratio blades, the beam-type finite element is the better choice.

Various finite beam elements for pretwisted blades have been developed. Most of them are derived from the differential equations of motion based upon a linear theory for the deformation of a rotating pretwisted blade proposed by Houbolt and Brooks[1]; for example, Lang and Nemat-Nasser[2] and Chen and Dugundji.[3] Since these finite elements assume the existence of a set of differential equations, their derivations cannot be conveniently extended to study cases with nonlinear material and geometrical influences or complicated dynamic motions. Recently, Downs[4] derived a beam stiffness matrix based on the matrix force method. By using the matrix force method the stiffening effect due to rotational motion does not arise naturally from the kinetic energy. This will restrict the approach to rotors with simple motions.

In the present paper, a more fundamental approach is presented to derive the finite element model matrices for the study of the vibration characteristics of nonuniform rotor blades. Finite element technique and the modified beam theory proposed by Downs[4] constitute the bases for the formulation. Instead of employing differential equations of motion to obtain finite element matrices, the model matrices are directly developed from the basic mechanics in terms of potential and kinetic energies of a pretwisted beam using the matrix displacement method. This approach premits easy inclusion of effects that are usually not taken into account in standard beam theory such as shear deformation, warping, and initial strain. The dynamic matrices are obtained systematically from the kinetic energy expression. This provides the capability of studying the effects of complicated

Received May 1, 1983; presented as Paper 83-0917 at the AIAA/ASME/ASCE/AHS 24th Structures, Structural Dynamics and Materials Conference, Lake Tahoe, Nev., May 2-4, 1983; revision received Nov. 16, 1983.

*George M. Bond Professor, Mechanical Engineering Department. Associate Fellow AIAA.

†Professor, Mechanical Engineering Department.

rotational motion of the blade such as gyroscopic precession. Only the derivation of matrices based upon linear beam theory is shown in this paper. Illustrative examples are presented comparing results with available data and other numerical solutions from rotating and nonrotating force fields.

Stiffness Matrix

Elementary beam theory cannot be directly applied to the study of twisted blade motion. The modification to beam theory employed in this paper was proposed by Downs.[4] The stiffness matrix of a twisted beam element is derived by assuming that the undeformed blade is pretwisted along its length about a straight longitudinal axis through shear centers of cross sections. These cross sections are parallel to the rotor-fixed x-y plane (see Fig. 1). Usually "principal coordinates" are assumed to be measured along axes having an origin at the centroid. Our coordinate axes, passing through the shear center, then would be parallel to the principal axes. The blade surface is supposed to be composed of helical fibers. If the position of an arbitrary point in a cross section is indicated by its principal coordinates ξ and η, the distance of this point from the shear center is

$$d=(\xi^2+\eta^2)^{1/2} \tag{1}$$

By designating α as the initial twist of the blade in radians per unit length and considering a portion of the blade with unit length, any helical fiber of length ℓ_H which is at a distance d from the centroid forms a small spiral angle γ (see Fig. 2) with the longitudinal axis. The length of this helical fiber can be approximated by

$$\ell_H=(1+\alpha^2 d^2)^{1/2} \tag{2}$$

Knowing this length, the axial strains of a helical fiber due to bending, axial force, and torsion can be determined. The filament strain caused by an axial extension of "a" per unit beam length is

$$\epsilon_a=\frac{[(1+a)^2+\alpha^2 d^2]^{1/2}-[1+\alpha^2 d^2]^{1/2}}{[1+\alpha^2 d^2]^{1/2}} \tag{3}$$

Neglecting higher order terms in α, this equation may be reduced to

$$\epsilon_a=a(1-\tfrac{1}{2}\alpha^2 d^2) \tag{4}$$

The filament strain due to an elastic twist $\bar{\phi}$ per unit beam length in the axial direction may be obtained in a similar manner

$$\epsilon_\phi=\bar{\phi}\alpha d^2(1-\tfrac{1}{2}\alpha^2 d^2) \tag{5}$$

The total strain in the axial direction from extension, bending, and torsion can be expressed as

$$\epsilon=(1-\tfrac{1}{2}\alpha^2 d^2)\left[\frac{\partial w}{\partial\zeta}-\xi^*\frac{\partial^2 u}{\partial\zeta^2}-\eta^*\frac{\partial^2 v}{\partial\zeta^2}+\frac{\partial\phi}{\partial\zeta}\alpha d^2\right] \tag{6}$$

where u and v are the deformations in the principal directions. The distance of an arbitrary point from the centroid is given by

$$\xi^*=\xi-e_x, \qquad \eta^*=\eta-e_y \tag{7}$$

where e_x and e_y are the positions of the neutral axis from shear center in the principal directions.

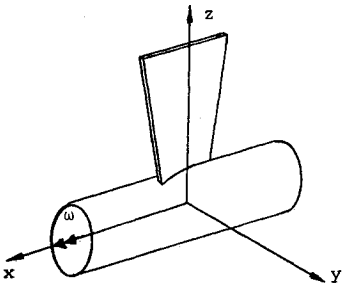

Fig. 1 Coordinate system fixed to a spinning rotor.

In the axial strain equation (6) the Euler assumption is made for the beam bending. If warping, shear deformation, or a higher order beam theory are to be considered in the analysis, Eq. (6) can be expanded to reflect these additional effects. Since shearing strain was not included in Eq. (6), the standard St. Venant torsional rigidity has to be added to the final stiffness matrix. The $\frac{1}{2}\alpha^2 d^2$ term in Eq. (6) represents the effect of substantial pretwist. The axial strain expression (6) is only valid for blades with thin cross section (i.e., a thickness ratio on the order of 5%). For a general cross section, a more comprehensive twisted beam theory is required such as the one proposed recently by Rosen.[5] The finite element approach presented in this paper can be expanded to include the evaluation of the torsional stress function required in such a theory.

The potential energy is equal to the strain energy stored in the blade and it is represented by the volume integration

$$U=\frac{1}{2}\int_{\text{Vol}}\{\sigma\}^T\{\epsilon\}\,\text{d Vol} \tag{8}$$

where $\{\epsilon\}$ is the deformation strain and $\{\sigma\}$ its corresponding stress. After substituting the axial strain given by Eq. (6) into Eq. (8) the stiffness matrix is obtained from the above integration. The integrand in Eq. (8) may be written in matrix form as

$$\{\sigma\}^T\{\epsilon\}=E(1-\tfrac{1}{2}\alpha^2 d^2)^2\begin{Bmatrix}\frac{\partial w}{\partial\zeta}\\ \frac{\partial^2 u}{\partial\zeta^2}\\ \frac{\partial^2 v}{\partial\zeta^2}\\ \frac{\partial\phi}{\partial\zeta}\end{Bmatrix}^T \times \begin{bmatrix} 1 & -\xi^* & -\eta^* & \alpha d^2 \\ & \xi^{*2} & \xi^*\eta^* & -\xi^*\alpha d^2 \\ \text{SYM} & & \eta^{*2} & -\eta^*\alpha d^2 \\ & & & \alpha^2 d^4 \end{bmatrix} \begin{Bmatrix}\frac{\partial w}{\partial\zeta}\\ \frac{\partial^2 u}{\partial\zeta^2}\\ \frac{\partial^2 v}{\partial\zeta^2}\\ \frac{\partial\phi}{\partial\zeta}\end{Bmatrix} \tag{9}$$

or

$$\{\sigma\}^T\{\epsilon\}=E(1-\tfrac{1}{2}\alpha^2 d^2)^2\{Du\}^T[P]\{Du\} \tag{9a}$$

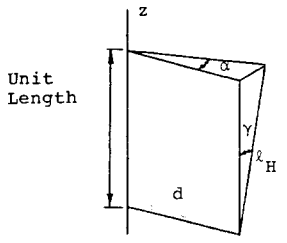

Fig. 2 Twisted fiber segment.

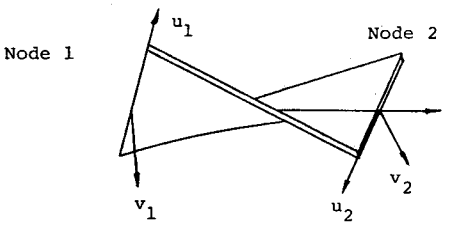

Fig. 3 Principal nodal displacements in bending.

For the finite element formulation, the deformations within an element have to be expressed in terms of nodal displacements. This is accomplished by assuming reasonable distributions for the element deformations and relating these deformations to nodal displacements by shape functions. Element bending deformations u and v in Eq. (9) are in the principal directions of the cross section and, hence, they rotate with the pretwist angle along the longitudinal axis (see Fig. 3). This leads to complicated finite element shape functions. In order to keep the shape functions simple, the displacements $\bar{u}$ and $\bar{v}$ in the element midplane principal directions are selected to represent the element bending deformations. The bending curvatures at an arbitrary cross section in $\{Du\}$ of Eq. (9) are related to curvatures in midplane coordinates by

$$\frac{\partial^2 u}{\partial \zeta^2} = \frac{\partial^2 \bar{u}}{\partial s^2}\cos\alpha s + \frac{\partial^2 \bar{v}}{\partial s^2}\sin\alpha s$$

$$\frac{\partial^2 v}{\partial \zeta^2} = \frac{\partial^2 \bar{u}}{\partial s^2}\sin\alpha s + \frac{\partial^2 \bar{v}}{\partial s^2}\cos\alpha s \qquad (10)$$

The coordinate s originates from the midplane of an element. Polynomials are employed to approximate the displacements

$$w = C_1 + C_2 s, \qquad \bar{u} = C_3 + C_4 s + C_5 s^2 + C_6 s^3$$

$$\bar{v} = C_7 + C_8 s + C_9 s^2 + C_{10} S^3, \qquad \phi = C_{11} + C_{12} s \qquad (11)$$

After determining the constants C_i in terms of nodal displacements, the strains $\{Du\}$ in Eq. (9) can be expressed in terms of nodal displacements by employing Eqs. (10) and (11). This can be written in matrix form as

$$\{Du\} = [T_1]\{u_i\} \qquad (12)$$

where $\{u_i\}$ represents the nodal displacement variables at the end nodes (*1* and *2*)

$$\{u_i\}^T = \left\{w_1, \frac{\partial u_1}{\partial \zeta}, u_1, \frac{\partial v_1}{\partial \zeta}, v_1, \phi_1, w_2, \frac{\partial u_2}{\partial \zeta}, u_2, \frac{\partial v_2}{\partial \zeta}, v_2, \phi_2\right\} \qquad (13)$$

and the elements in matrix $[T_1]$ are functions of the pretwist angle per length α and element axial coordinate s.

Substituting Eqs. (12) and (9) into the potential energy expression (8), the stiffness matrix is attained from the integration

$$[K] = \int_{\text{Vol}} [S]\,dV \qquad (14)$$

with

$$[S] = E(1-\alpha^2 d^2)\,[T_1]^T[P]\,[T_1] \qquad (15)$$

The size of stiffness matrix $[K]$ is 12×12.

To extend the integration [Eq. (14)] of the stiffness matrix for a relatively complex cross section representative of actual blades requires the introduction of a method known as the isoparametric formulation in the finite element analysis. This involves the distortion of a simple square area into areas of arbitrary shapes. The accuracy of the "mapping" into distorted shape in the manner dictated by the actual blade depends on the number of nodes introduced around the circumference. In this paper all results are based on eight boundary nodes. In the standard isoparametric formulation of three-dimensional distortion, mapping takes place in all three directions. In the present application, the integral equation (14) of the stiffness matrix already contains the blade pretwist effect. Therefore, it suffices to perform distortion in two dimensions of the blade cross-sectional area only. This reduces the amount of required numerical computation in evaluating the stiffness matrix. Following the standard procedure for quadratic isoparametric elements, the principle coordinates of the cross section can be approximated by

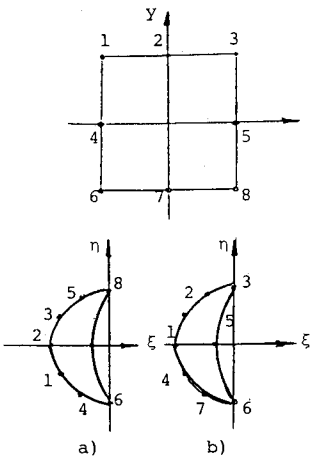

Fig. 4 Crescent cross section.

$$\xi = N_1\xi_1 + N_2\xi_2 + \ldots + N_8\xi_8$$

$$\eta = N_1\eta_1 + N_2\eta_2 + \ldots + N_8\eta_8 \qquad (16)$$

with ξ_i and η_i representing the nodal positions of N_i the shape functions. After the transformation of coordinate systems by Eq. (16), the integration (14) is evaluated through matrix $[S']$ in the distorted coordinate system with the Jacobian transformation matrix $[J]$

$$[K] = \int_{\text{Vol}} [S']\det[J]\,d\ \text{Vol} \qquad (17)$$

In order to establish the accuracy of this numerical approach, the static deflections of uniform cantilever beams with different cross sections were investigated. For several elliptical and triangular cross sections, the error in computed free end deflections using six finite elements remained below 3% of the beam solution. Another example investigated is the cross section defined by a convex and a concave edge and shaped like a crescent (see Fig. 4). Two nodal distribution

schemes were tested. They are shown in Figs. 4a and 4b. For a cantilever beam with load applied at the shear center of the free end, the vertical and horizontal free end deflections were compared. It was shown that the eight nodes in Fig. 4b are better placed than the ones in Fig. 4a. The placement of nodes around the circumference is very sensitive. If there were only three nodes along the circular edge the results were as much as 100% in error. This reflects the fact that a three-node parabolic interpolation cannot represent the edge consisting of a large angle circular arc correctly.

For a twisted blade with a uniform rectangular cross section, some experimental results were presented by Carnegie.[6] In these experiments the blades were uniformly pretwisted over a length of 15.24 cm with cross-sectional dimensions of 2.54×0.1587 cm. The blade material was mild steel. Using these blade data and six finite element segments the static deflection under unit load at the tip was computed. The results are compared to Carnegie's experimental results in Fig. 5. The vertical and horizontal deflections are plotted vs the total pretwist angle α_L. The present solution is almost identical to theoretical solutions provided by Carnegie in Ref. 6. Obviously there are many ways to calculate the structural stiffness of a pretwisted uniform beam.

Kinetic Energy

For rotating blades the kinetic energy expression

$$T = \frac{1}{2}\rho \int_{\text{Vol}} v^2 \, dV \tag{18}$$

determines the mass matrix of the equation of motion, the dynamic correctional effect on the structural stiffness matrix, and the blade motion induced forces. According to finite element formulation, the kinetic energy integration is evaluated at each element. This leads to element model matrices which are assembled to represent the kinetic energy.

Beginning with the displacement vector r of an arbitrary point in the element fixed ijk coordinate system, the vector is measured from the center of the rotor.

$$r = (\xi + u - \eta\phi)i + (\eta + v + \xi\phi)j + \left\{ z + \zeta + w - \xi^* \frac{\partial u}{\partial \zeta} - \eta^* \frac{\partial v}{\partial \zeta} + \alpha d^2 \phi - \frac{1}{2}\int_R^\zeta \left[\left(\frac{\partial u}{\partial \zeta}\right)^2 + \left(\frac{\partial v}{\partial \zeta}\right)^2 \right] d\zeta - \frac{1}{2}(\xi^2 + \eta^2)\int_R^\zeta \left(\frac{\partial \phi}{\partial \zeta}\right)^2 d\zeta \right\} k \tag{19}$$

R is the rotor hub radius. The z displacement component includes the "foreshortening" terms[7,8] due to both bending deflections and torsional rotations. These terms were not included in the axial strain expression (6) because they are of higher order and do not effect the linear stiffness matrix. Also the $\frac{1}{2}\alpha^2 d^2$ factor representing substantial pretwist in Eq. (6) is neglected in the displacement due to higher order effects. A proper displacement expression such as Eq. (19) is essential in order to obtain the correct model matrices from the kinetic energy.

Following Eq. (19) the velocity of the same element arbitrary point can be obtained

$$v = (\dot{u} - \eta\dot{\phi})i + (\dot{v} + \epsilon\dot{\phi})j + \left\{ \dot{\omega} - \xi^* \frac{\dot{\partial u}}{\partial \zeta} - \eta^* \frac{\dot{\partial v}}{\partial \zeta} + \alpha d^2 \dot{\phi} - \int_R^\zeta \left[\frac{\partial u}{\partial \zeta}\frac{\dot{\partial u}}{\partial \zeta} + \frac{\partial v}{\partial \zeta}\frac{\dot{\partial v}}{\partial \zeta} \right] d\zeta - d^2 \int_R^\zeta \frac{\partial \phi}{\partial \zeta}\frac{\dot{\partial \phi}}{\partial \zeta} d\zeta \right\} k + \omega \times r \tag{20}$$

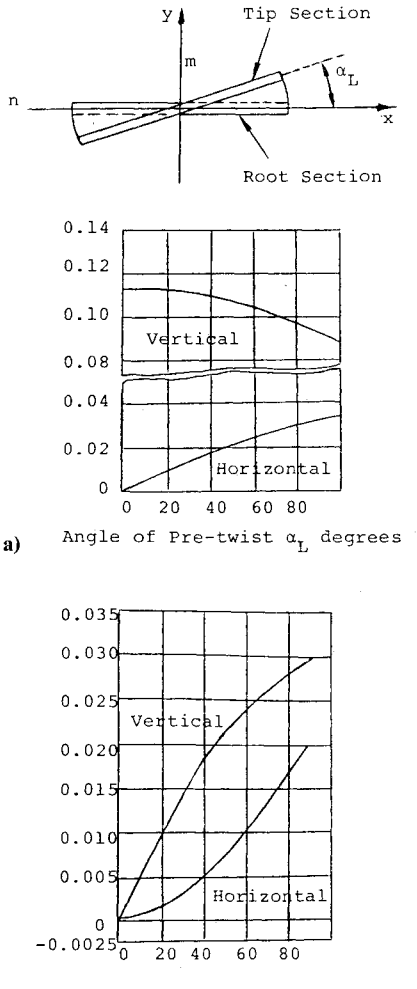

Fig. 5 Static deflections of rectangular cross-sectional beams under concentrated loading (six elements): a) load applied vertically, b) load applied horizontally.

where ω represents the angular velocity of the element coordinate system. For the simple case associated with rotor spin, ω is the angular velocity of the rotor. An example involving more complicated rotor motion can be found in Ref. 9.

The deformation variables employed in Eqs. (19) and (20) are

$$\{u_E\}^T = \left\{ u,\ v,\ w,\ \phi,\ \frac{\partial u}{\partial \zeta},\ \frac{\partial v}{\partial \zeta},\ \frac{\partial \phi}{\partial \zeta} \right\} \tag{21}$$

and their time derivatives. They are located in the element coordinate system fixed to the element midplane. In order for the model matrices derived from the kinetic energy to be consistent with the structural stiffness matrix, the deformation variables (21) in the velocity expression (20) have to be the same as those employed for the stiffness matrix. Repeating the procedure that derived Eq. (12) in the stiffness matrix formulation, the variables $\{u_E\}$ in Eq. (20) can be expressed in terms of nodal deformation variables $\{u_i\}$ by

$$\{u_E\} = [T_2]\{u_i\} \tag{22}$$

Finally, with Eq. (22), the velocity of Eq. (20) is substituted into the kinetic energy equation (18) to obtain the following

matrix equation:

$$T=\frac{1}{2}\rho\int_{\text{Vol}}\{\{\dot{u}_i\}[M_1]\{\dot{u}_i\}+\{u_i\}[M_2]\{u_i\}+\{\dot{u}_i\}[M_3]\{u_i\}+\{M_4\}^T\{\dot{u}_i\}+\{M_5\}^T\{u_i\}\}\text{d Vol} \quad (23)$$

The model matrices $[M_i]$ are defined as

$$[M_i]=[T_2]^T[A_i][T_2] \qquad i=1,2,3$$

$$\{M_i\}=[A_i][T_2] \qquad i=4,5 \quad (24)$$

Matrices $[A_i]$ represent different parts of the square of the velocity expression (20). Details of the derivation can be found in Ref. 7. To perform the integration in Eq. (23) for arbitrary cross section, the numerical distortion procedure employed in the evaluation of the stiffness matrix can be applied here as well.

Knowing both kinetic and potential energies the equations of motion can be established via Lagrange's equation. The mass matrix is obtained after integrating matrix $[M_1]$. Due to the effect of pretwist this mass matrix is slightly different from the standard consistent mass matrix of a beam element. The elements of matrix $[M_2]$ after integration represent the changes in stiffness due to rotational motion. This matrix is sometimes referred to as the dynamic stiffness matrix. It is combined with the structural stiffness matrix of Eq. (14) to form the combined effective stiffness matrix. Matrix $[M_3]$ does not affect the equations of motion. The forcing terms of the equations of motion are determined by matrices $\{M_4\}$ and $\{M_5\}$. For the simple case of a rotor spinning about one axis, the matrix $\{M_4\}$ is zero.

Numerical Examples

The accuracy of the proposed beam element was studied by comparing the natural frequencies with those obtained from the finite element analysis using NASTRAN. The NASTRAN results were obtained by MacBain[10] using 230 plate elements. The following mild steel blade example was calculated: length, $\ell=17.78$ cm; width, $w=7.62$ cm; and thickness, $t=0.229$ cm. In Fig. 6, the first, second, and third bending frequencies and the first and second torsional frequencies at zero rotor spin velocity are plotted vs the total pretwist angle of the blade and compared with the NASTRAN solution. In Fig. 7, the same frequencies with 30 deg pretwist angle are plotted vs the rotational speed. In this case the blade setting angle is zero and the hub radius is 17.78 cm.

The numerical results obtained with six beam elements indicate that the beam formulation predicts acceptable accuracy for the five lowest natural frequencies. The accuracy is better in the nonrotating caes. Considering the differences in required amounts of computer memory and computation time, the beam solution is quite attractive. The same examples were used by Chen and Dugundji[3] to show the accuracy of a twisted beam finite element derived from the governing differential equations of motion provided by Houbolt and Brooks.[1] For a twisted beam with thin cross section, the theoretical assumptions made by Houbolt and Brooks are very similar to those made in this paper with little difference in the calculated natural frequency.

Another twisted beam theory was proposed in Ref. 11, although the method is more of "preliminary design" nature. Our improved beam finite element was tested against several

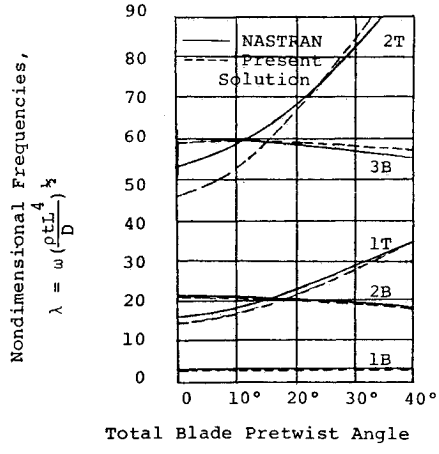

Fig. 6 Natural frequencies vs pretwist angle.

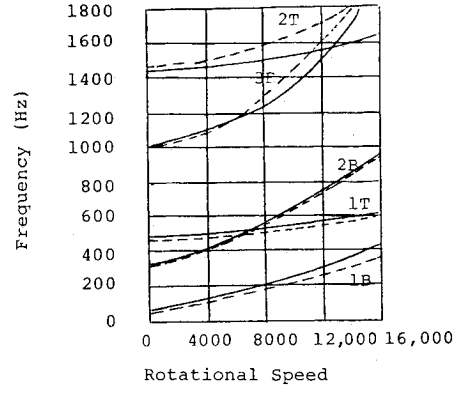

Fig. 7 Natural frequency vs rotational speed (30 deg pretwist angle).

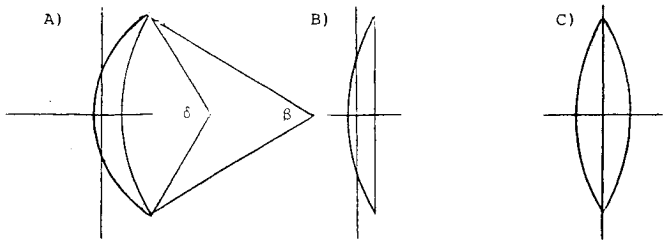

Table 1 Beam deformations in centrifugal force field (6 elements)[a]

Cross section	δ, deg	β, deg	Angular rotation ϕ, rad	Bending displacement u, cm	v, cm
A	34.12	11.44	0.0054	0.2271	−0.3505
B	22.8	0	0.0117	0.1352	−0.2113
C	11.44	−11.44	0.0184	0	0

[a] Rotor spin: 5000 rpm, hub radius 17.78 cm, blade length 17.78 cm, maximum thickness 0.254 cm, chord 5.08 cm, base setting angle −15 deg, total pretwist angle −45 deg, material: mild steel.

sample problems from Ref. 9 and, in all significant respects, has been shown to deliver results that are closer to the more exact solutions obtained from a two-dimensional finite element program (NONSAP).

A final example has been included to show the convenience of using the pretwisted finite beam element. The elastic twist (untwist) attributable to centrifugal loading of a pretwisted blade has been studied for a sequence of three geometries. In every case the pretwist axis coincides with the shear center of the cross section and is taken to be initially radial. The results, shown in Table 1, demonstrate the capability of the method to predict accurately the elastic twist of a cantilever rotor blade as well as the bending displacements. Although these deformations are in response to the centrifugal force field in this example, it is a simple matter to include the effect of steady aerodynamic loading (force and moment) if these loads are specified. A comparison with much more time-consuming NASTRAN computation is again quite favorable and the method can be adapted to other choices of pretwist (or stacking) axes.

A true test of a finite element for pretwisted blades does not only rest with prediction of dynamic behavior in a centrifugal force field. The same method must be able to generate dynamic effects due to more complicated blade geometry, such as blade lean (nonradial line of centroids), properly. The model matrices for this case presently are being developed.

The technique employed in the present method to derive dynamic model matrices directly from the potential and kinetic energies might as well be applied to linear plate and shell-type finite elements. This would eliminate the required iteration step in present two-dimensional finite element analysis.

Conclusions

The development of a finite element for pretwisted blades, based on beam theory, has been presented. The effects of dynamic motion on blade properties are derived systematically from the potential and kinetic energy expressions. The dynamic model matrices, including the mass matrix, the correctional matrix to the structural stiffness matrix, and the forcing terms are obtained. Comparing the derivation of model matrices with other beam element theory, the present approach is thought to be more fundamental. The evaluation of cross-sectional properties is performed directly based on area shape. All model matrices are computed numerically in a straightforward fashion.

To determine the accuracy of this theory three different types of sample problems were selected. Pretwisted beams under static load were used to test the accuracy of the the structural stiffness matrix. Examples of natural frequency determination in rotating and nonrotating force fields serve to demonstrate the accuracy of the mass matrix and the motion-induced correctional stiffness matrix. Finally, the forcing in the equations of motion is studied by computing the deformations of the pretwisted blade under centrifugal loading.

It is interesting to note that, due to rotational (centrifugal) effects, a typical pretwisted blade is subjected to a radial body force as well as a twisting moment about the longitudinal axis. The radial force contribution causes the pretwisted blade to untwist, and, hence, reduce the angle of twist. For most pretwisted configurations, in terms of setting angle, positive or negative initial pretwist, the twisting moment contribution tends to increase the angle of twist. Whether a pretwisted blade in a centrifugal force field will experience a net untwist depends on which of these two loadings dominates.

Acknowledgment

These studies have been supported under a research grant from NASA Lewis Research Center, with Robert E. Kielb as Technical Officer.

References

[1] Houbolt, J. C. and Brooks, G. W., "Different Equations of Motion for Combined Flapwise Bending, Chordwise Bending, and Torison of Twisted Nonuniform Blades," NACA TN 3905, 1958.

[2] Lang, K. W. and Nemat-Nasser, S., "An Approach for Estimating Vibration Characteristics of Nonuniform Rotor Blades," *AIAA Journal*, Vol. 17, Sept. 1979, pp. 995-1002.

[3] Chen, L. T. and Dugundji, J., "Investigation of the Vibration Characteristics of Shrouded Bladed Disk Rotor Stages," *Journal of Aircraft*, Vol. 17, July 1980, pp. 141-146.

[4] Downs, B., "The Effect of Substantial Pretwist on the Stiffness Properties of Thin Beams of Cambered Section," *Journal of Applied Mechanics*, Vol. 46, June 1979, pp. 341-344.

[5] Rosen, A., "Theoretical and Experimental Investigation of the Nonlinear Torsion and Extension of Initially Twisted Bars," *Journal of Applied Mechanics*, Vol. 50, June 1983, pp. 321-326.

[6] Carnegie, W., "Static Bending of Pretwisted Cantilever Blading," *Proceedings of the Institute of Mechanical Engineers*, Vol. 171, No. 32, 1957, pp. 873-893.

[7] Vigneron, F. R., "Comment on Mathematical Modeling of Spinning Elastic Bodies for Modal Analysis," *AIAA Journal*, Vol. 13, Jan. 1975, pp. 126-127.

[8] Kaza, K. R. V. and Kielb, R. E., "Coupled Bending-Bending-Torsion Flutter of a Mistuned Cascade with Nonuniform Blades," *Proceedings of the 23rd AIAA/ASME/ASCE/AHS Structures, Structural Dynamics and Materials Conference*, New Orleans, La., May 1982, pp. 446-461.

[9] Sisto, F. and Chang, A. T., "The Influence of Gyroscopic Forces on the Dynamic Behavior and Flutter of Rotating Blades," Stevens Rept. ME-RT-82006 prepared for NASA Lewis Cleveland, Ohio, Aug. 1982.

[10] MacBain, J. C., "Vibration Behavior of Twisted Cantilevered Plates," *Journal of Aircraft*, Vol. 12, No. 4, April 1975, pp. 343-349.

[11] Durocher, L. L. and Kane, J., "A Preliminary Design Tool for Pretwisted, Tapered Beams or Turbine Blades," *Journal of Mechanical Design*, Vol. 102, Oct. 1980, pp. 742-748.